Supplemental Information For:

Outdoor chloramines and chlorine levels detected and elevated near an indoor sports complex

Andrea A. Angelucci[a], Leigh R Crilley[a], Rob Richardson[b], Thalassa S. E. Valkenburg[b], Paul S. Monks[b], James M. Roberts[c], Roberto Sommariva[b,*], and Trevor C. VandenBoer[a,*]

[a]Department of Chemistry, York University, Toronto, ON, Canada

[b]Department of Chemistry, University of Leicester, Leicester, UK.

[c]Chemical Sciences Laboratory, National Oceanic and Atmospheric Administration, Boulder, CO, USA

*Communicating Author Contact: tvandenb@yorku.ca; rs445@le.ac.uk

S1. NH_2Cl interference on m/z 162 and 164 channels

The m/z 162 and 164 channels correspond to the $[I{\cdot}Cl]^-$ cluster, which can be attributed to the fragmentation pattern of chlorine-containing compounds. Other possible candidates are hydrochloric acid (HCl) and nitryl chloride ($ClNO_2$) and ClNO. Figure S1 shows that the primary cluster peak of HCl is that of $[I{\cdot}HCl]^-$ (m/z 163, 165) and not $[I{\cdot}Cl]^-$, as such we can conclude that HCl is not responsible for the m/z 162 and 164 signal seen in these measurements. A signal at m/z 162 and 164 does originate from $ClNO_2$, as well as at m/z 208 and 210, with the latter corresponding to the $[I{\cdot}ClNO_2]^-$ cluster. One would expect the counts from both sets of channels to be correlated if they both originate from the same molecule however here this is not the case (Figures S3-S4), suggesting an interference from another Cl^- containing molecule. ClNO could account for some of the observed signal at m/z 162, as the $[I{\cdot}ClNO]^-$ cluster will fragment to form $[I{\cdot}Cl]^-$ as NO has zero electron affinity. However, the contributions from ClNO are expected to be

small as its levels in the boundary layer are very low,[1] to the point that this contribution can be neglected. As such, the signal on the m/z 162 channel can be separated using the below equations.

$$ClNO_2\ Counts_{m/z\ 162} = ClNO_2(pptv)_{m/z\ 208} * ClNO_2\ Sensitivity\ (ncps/pptv)_{m/z\ 162} \quad \textbf{SE1}$$

$$Unknown\ Counts_{\ m/z\ 162} = Total\ Counts(ncps)_{m/z\ 162} - ClNO_2\ Counts_{m/z\ 162} \quad \textbf{SE2}$$

Figure S2 shows that the unknown signal at m/z 162 has an isotopic ratio similar to that of chlorine. Moderate correlation ($r^2 = 0.56$) is observed between the unknown portion of the m/z 162 signal and signal at m/z 178; the signal corresponding to the $[I{\cdot}NH_2Cl]^-$ cluster. This provides evidence of interference from NH_2Cl on the m/z 162 channel. This interference further supports the use of the m/z 208 channel to measure $ClNO_2$.

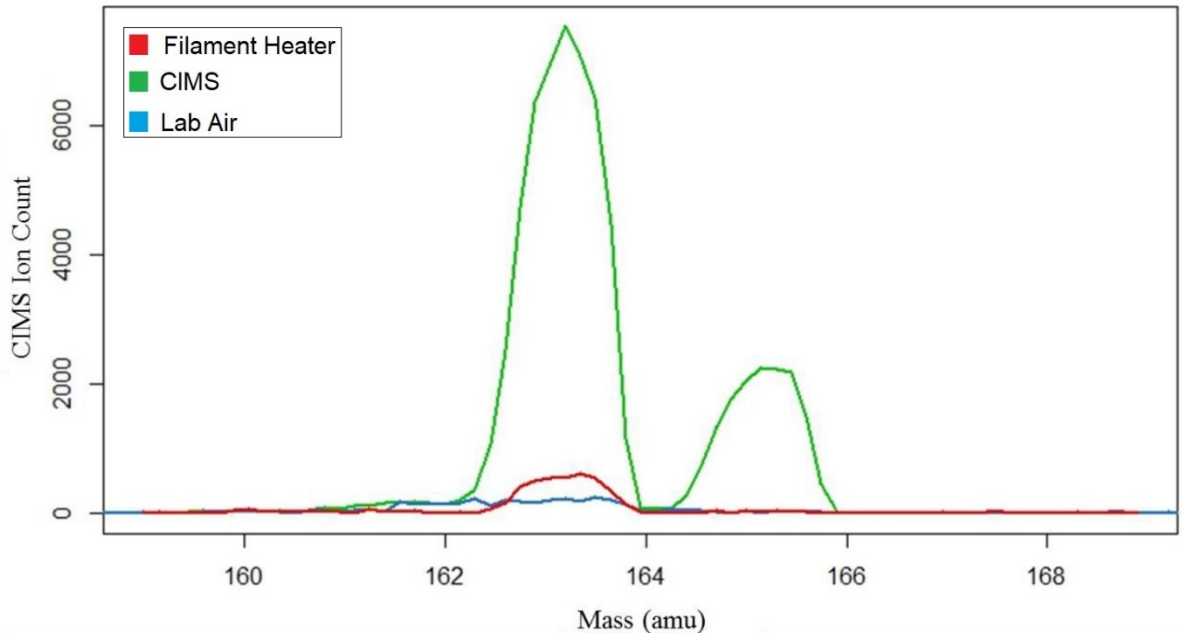

Figure S1: Hydrochloric acid cluster peak ([I·HCl]-) direct into the CIMS (green), through a filament heater that destroys HCl (red) and lab air reference (blue).

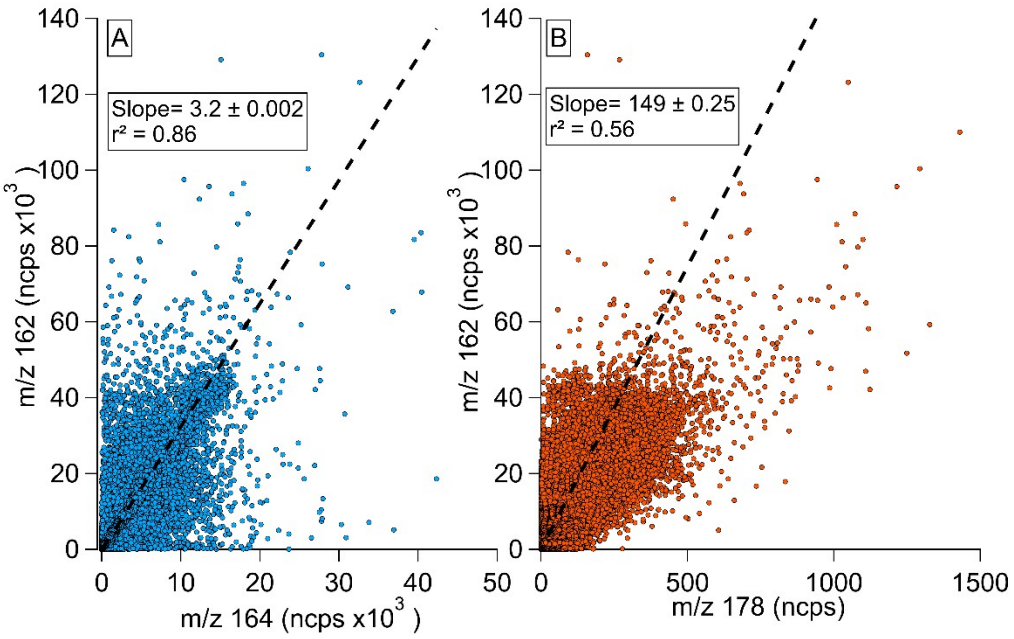

Figure S2: Normalized ion counts combined for both 2014 and 2016 AURN campaigns at m/z 164 from the unknown compound $[I \cdot Cl]^-$ correlated to counts at m/z 162 (Panel A) and correlation between m/z 162 and 178 (Panel B). Contribution from $ClNO_2$ has been removed from both m/z 162 and 164 depicted here. Correlation coefficient (r^2) values were calculated via orthogonal least-distance regression (black dashed line).

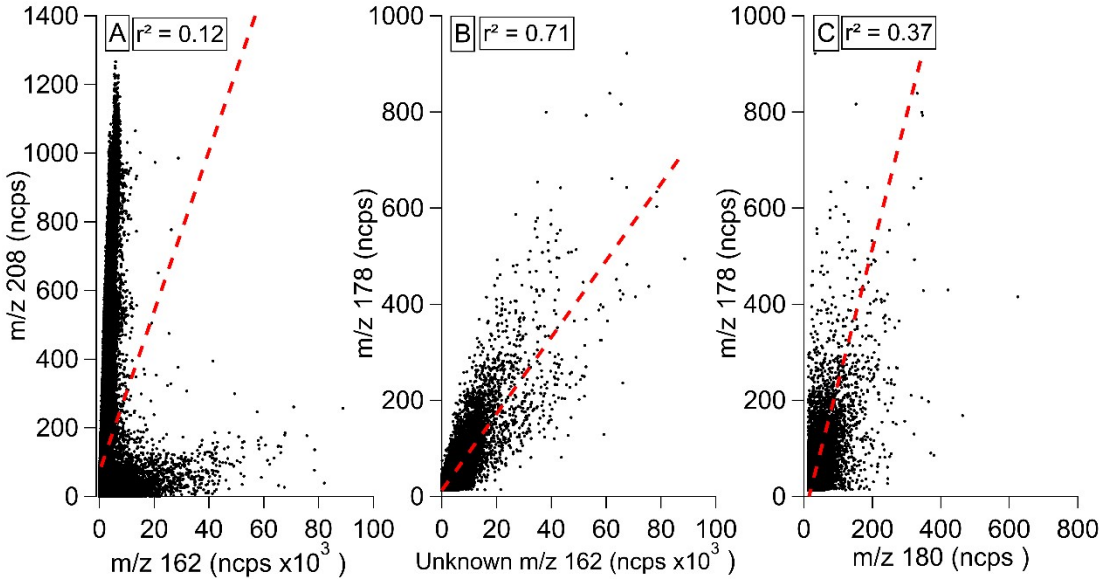

Figure S3: Correlation plots between (A) $[I \cdot ClNO_2]^-$ (208) and $[I \cdot Cl]^-$ (162),), (B) $[I \cdot ClNH_2]^-$ (178) and Unknown $[I \cdot Cl]^-$ (162), and (C) $[I \cdot ClNH_2]^-$ (178/180) for the 2014 AURN campaign. Correlation coefficient (r^2) values were calculated via orthogonal least-distance regression (red dashed line).

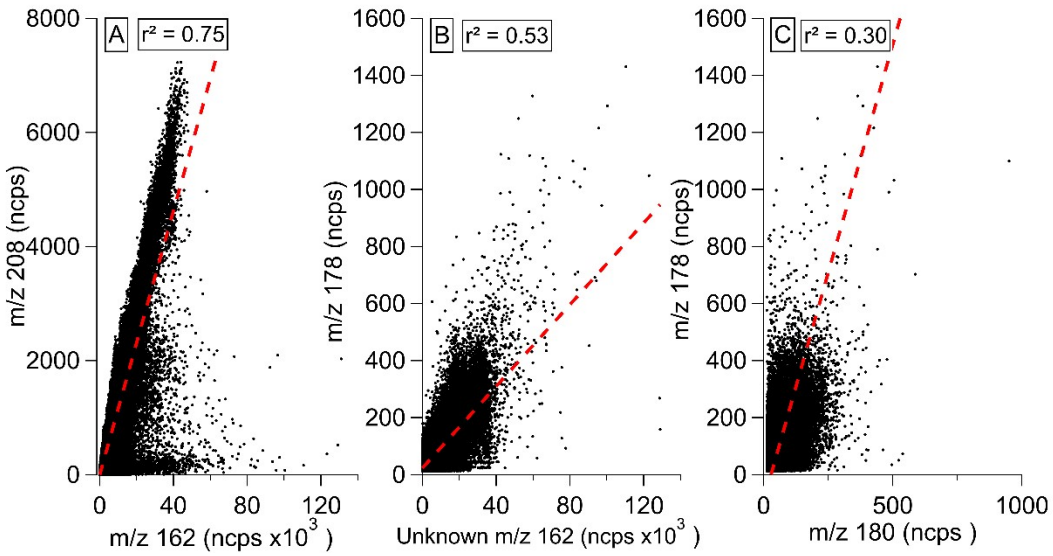

Figure S4: Correlation plots between (A) $[I{\cdot}ClNO_2]^-$ (208) and $[I{\cdot}Cl]^-$ (162),), (B) $[I{\cdot}ClNH_2]^-$ (178) and Unknown $[I{\cdot}Cl]^-$ (162), and (C) $[I{\cdot}ClNH_2]^-$ (178/180) for the 2016 AURN campaign. Correlation coefficient (r^2) values were calculated via orthogonal least-distance regression (red dashed line).

S2. Ambient Measurements – Part 1: Identifying Chloramines

Table S1: Isotopic ratios of outdoor $[I{\cdot}Cl]^-$, $[I{\cdot}NH_2Cl]^-$, and $[I{\cdot}Cl_2]^-$ clusters derived from slope. Errors displayed for each ratio are one standard deviation (σ).

	m/z 162/164 **$[I{\cdot}Cl]^-$**	**m/z 178/180** **$[I{\cdot}NH_2Cl]^-$**
Theoretical Ratio	3.13	3.13
AURN 2014-Slope	3.76±0.006	2.79±0.024
r^2	0.72	0.37
AURN 2016-Slope	3.23±0.004	3.20±0.021
r^2	0.85	0.30

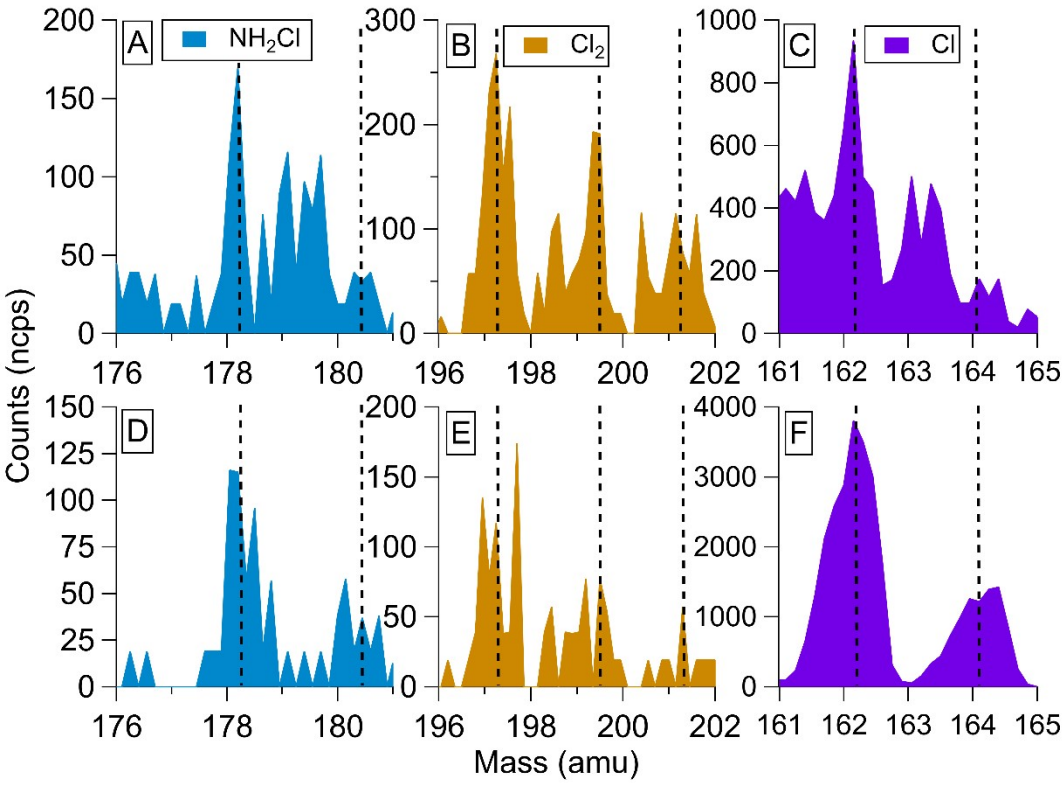

Figure S5: Normalized counts per second (ncps) for ions in selected ambient mass spectra of NH_2Cl (A), Cl_2 (B), and Cl (C) in 2014 and in 2016 (D, E and F). Black dashed lines indicate the mass of the ^{35}Cl and ^{37}Cl isotopes. 2014 data was taken from August 17 at 18:06 (A), 21:06 (B), 12:06 (C); while 2016 data was from February 14 at 07:14 (D), 12:14 (E), 04:14 (F).

S3. Chloramine calibration of experiments

Gas-phase chloramines were synthesized using the following procedure. A solution of $(NH_4)_2SO_4$ was added to a cylindrical glass reactor (16 x 3 cm) filled with glass beads. The reactor was rotated and shaken to ensure all beads were covered in solution and then left to dry overnight under dry air (2 L min^{-1}). After drying, the reactor full of dried $(NH_4)_2SO_4$ solution was placed into the calibration setup (Figure S6). A mix of humidified air and Cl_2 (calibration standard BOC, 5 ppmv) was flowed through the reactor, generating chloramines via reaction with NH_4SO_4, according to the reactions SR1-3 (see below). The reactions of Cl_2 to form NH_2Cl, $NHCl_2$, and NCl_3 result in an overall reaction stoichiometry is 1:2:3 for NH_2Cl: $NHCl_2$:NCl_3 with respect to Cl_2.

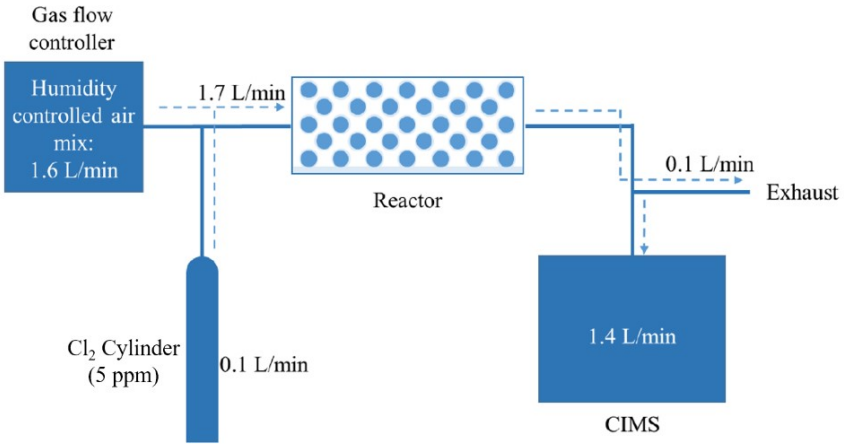

Figure S6: Experimental setup for chloramine generation calibration experiments. Solid lines indicate connections, dashed arrows indicate direction of gas mix flow.

$$Cl_2 + H_2O \rightarrow HOCl + HCl$$
$$(NH_4)_2SO_4 + H_2O \rightarrow 2NH_3 + H_2SO_4 + H_2O$$
$$NH_3 + HOCl \rightarrow ClNH_2 \rightarrow + H_2O$$

$$\mathbf{Cl_2} + (NH_4)_2SO_4 \rightarrow \mathbf{ClNH_2} + HCl + H_2SO_4 + NH_3 \quad \textbf{(SR1)}$$

$$Cl_2 + H_2O \rightarrow HOCl + HCl$$
$$(NH_4)_2SO_4 + H_2O \rightarrow 2NH_3 + H_2SO_4 + H_2O$$
$$NH_3 + HOCl \rightarrow ClNH_2 \rightarrow + H_2O$$
$$Cl_2 + H_2O \rightarrow HOCl + HCl$$
$$ClNH_2 + HOCl \rightarrow Cl_2NH + H_2O$$

$$\mathbf{2Cl_2} + (NH_4)_2SO_4 \rightarrow 2\ HCl + NH_3 + H_2SO_4 + \mathbf{Cl_2NH} \quad \textbf{(SR2)}$$

$$Cl_2 + H_2O \rightarrow HOCl + HCl$$
$$(NH_4)_2SO_4 + H_2O \rightarrow 2NH_3 + H_2SO_4 + H_2O$$
$$NH_3 + HOCl \rightarrow ClNH_2 \rightarrow + H_2O$$
$$Cl_2 + H_2O \rightarrow HOCl + HCl$$
$$ClNH_2 + HOCl \rightarrow Cl_2NH + H_2O$$
$$Cl_2 + H_2O \rightarrow HOCl + HCl$$
$$Cl_2NH + HOCl \rightarrow Cl_3N + H_2O$$

$$\mathbf{3Cl_2} + (NH_4)_2SO_4 \rightarrow 3\ HCl + NH_3 + H_2SO_4 + \mathbf{Cl_3N} \quad \textbf{(SR3)}$$

During the calibration, the levels of Cl_2 were changed stepwise (4 steps), at mixing ratios of 52, 93, 183, and 190 ppbv (Figure S7, circled areas), as well as a measurement of background signal at 0 ppbv. The outflow of the reactor was sampled for chloramines and Cl_2 using the I^- CIMS under the conditions described in the main manuscript for ambient sampling.

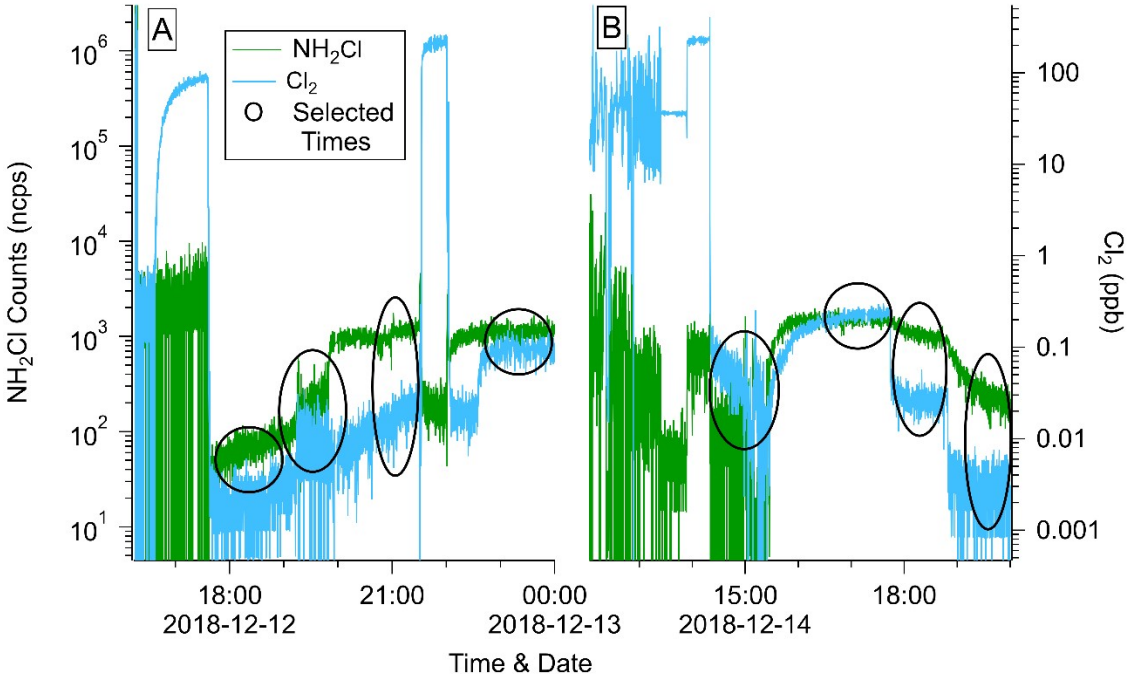

Figure S7: Timeseries of Cl_2 (blue) and NH_2Cl (green) for NH_2Cl calibration experiment from December 12 (A) and 14 (B) in 2018. Selected time periods used for calibration curves and ratio calculations have been denoted qualitatively with black circles.

The generated levels of chloramines can be quantified by determining the difference in measured Cl_2 after the reactor compared to the known amount of Cl_2 entering – calculated from the reported Cl_2 cylinder concentration after application of the dilution factor, assuming the reacted Cl_2 produced chloramines. During the calibration experiment, only NH_2Cl (at m/z of 178 and 180) was measured continuously by the CIMS, but this was complemented by regular (about every 60 mins) full mass spectral scans during each Cl_2 addition. In addition to NH_2Cl, both $NHCl_2$ and NCl_3 were also observed at measurable levels during the full mass spectral scans throughout the calibration (i.e. during each Cl_2 addition).

S4. Estimation of NH_2Cl, $NHCl_2$, & NCl_3 sensitivity

Here we estimate the quantity of the product compounds using known stoichiometry, as well as drawing from the results reported by Mattila *et al.*[2] To quantify the amount of chloramines produced using the known amounts of reacted Cl_2, the stoichiometry of the products relative to Cl_2 must be accounted for. This stoichiometry varied depending on which chloramine species was formed; with one, two and three Cl_2 molecules required for the formation of one NH_2Cl, $NHCl_2$ and NCl_3 molecule, respectively (See SR1-R3). In addition, the relative levels of each chloramine species were calculated using the raw counts in the full mass scans. The relative contributions of each chloramine species determined against the total signal of summed chloramine products (i.e. NH_2Cl + $NHCl_2$ + NCl_3) as a percentage. Overall, $NHCl_2$ gave the most abundant signal (97.66±0.44 %), followed by NH_2Cl (2.26±0.46 %) and NCl_3 (0.070±0.025 %) and this ratio was generally consistent (±1σ here) over several repeated experiments (Figures S8-9). Calculating the % NH_2Cl, % $NHCl_2$, and % NCl_3 was done using the full spectral scans of these experiments. Here, we calculated the % of each chloramine species under two scenarios to capture the potential range of I-CIMS sensitivity. First, we assumed an equal CIMS sensitivity towards all chloramines (1:1:1, SE3) and second based on Mattila *et al.,* we assumed the CIMS is 5x as sensitive to $NHCl_2$ as NH_2Cl and 5x as sensitive to NCl_3 as $NHCl_2$ (1:5:25, SE4-6).[2] The spectral scans were used exclusively for this calculation, as opposed to the timeseries data, as the latter data did not provide observations of $NHCl_2$ or NCl_3.

$$\%Chloramine\ Species\ (1{:}1{:}1) = \frac{Counts\ Of\ Specific\ Chloramine\ Species}{NH_2Cl\ Counts + DCA\ Counts + TCA\ Counts}$$

SE3

$$\%NH_2Cl\ (1{:}5{:}25) = \frac{NH_2Cl\ Counts}{NH_2Cl\ Counts + \frac{NHCl_2\ Counts}{5} + \frac{NCl_3\ Counts}{25}}$$

SE4

$$\%NHCl_2\ (1{:}5{:}25) = \frac{\frac{NHCl_2\ Counts}{5}}{NH_2Cl\ Counts + \frac{NHCl_2\ Counts}{5} + \frac{NCl_3\ Counts}{25}}$$

SE5

$$\%NCl_3\ (1{:}5{:}25) = \frac{\frac{NCl_3\ Counts}{25}}{NH_2Cl\ Counts + \frac{NHCl_2\ Counts}{5} + \frac{NCl_3\ Counts}{25}}$$

SE6

These relative chloramine quantities were then plotted against elapsed reaction time and fit to a linear equation (Figures S8-9) to determine how the evolution of the three species changed as the reaction time during the calibrations progressed.

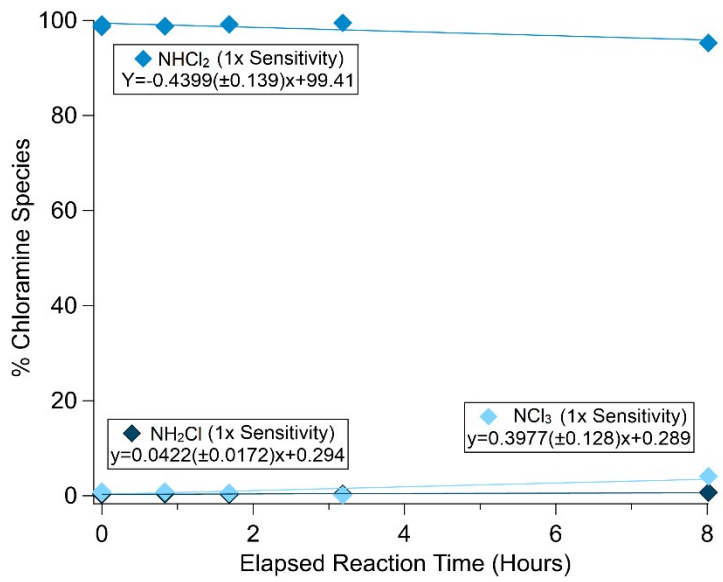

Figure S8: Timeseries of % monochloramine (NH_2Cl, dark blue), dichloramine ($NHCl_2$, blue), and trichloramine (NCl_3, light blue) for CIMS Calibration Experiments. These percentages assume an instrument sensitivity of 1:1:1 (NH_2Cl: $NHCl_2$:NCl_3).

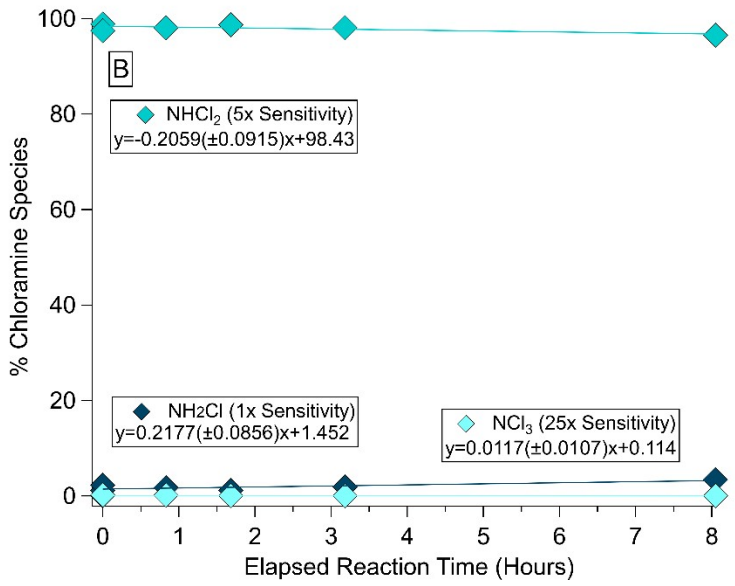

Figure S9: Timeseries of % monochloramine (NH_2Cl, dark blue), dichloramine ($NHCl_2$, blue), and trichloramine (NCl_3, light blue) for CIMS Calibration Experiments. These percentages assume a relative instrument sensitivity of 1:5:25 (NH_2Cl: $NHCl_2$/5:NCl_3/25).

Sensitivities were calculated by determining the reaction fate of Cl_2 with NH_2Cl, $NHCl_2$, and NCl_3 using the 1:2:3 stoichiometric ratio (SR1-3) while also considering the measured percentages of each chloramine species relative to each other (SE7-12). The percentage of each chloramine species used were those calculated previously through each of the linear equations (Figures S8-9).

$$Reacted\ Cl_{2Form\ NH_2Cl} = Reacted\ Cl_{2_{Total}} * \frac{\%\ NH_2Cl(1{:}1{:}1)/100}{1} \quad \text{SE7}$$

$$Reacted\ Cl_{2Form\ NHCl_2} = Reacted\ Cl_{2_{Total}} * \frac{\%NHCl_2\ (1{:}1{:}1)/100}{2} \quad \text{SE8}$$

$$Reacted\ Cl_{2Form\ NCl_3} = Reacted\ Cl_{2_{Total}} * \frac{\%NCl_3\ (1{:}1{:}1)/100}{3} \quad \text{SE9}$$

$$Reacted\ Cl_{2Form\ NH_2Cl} = Reacted\ Cl_{2_{Total}} * \frac{\%\ NH_2Cl(1{:}5{:}25)/100}{1} \quad \text{SE10}$$

$$Reacted\ Cl_{2Form\ NHCl_2} = Reacted\ Cl_{2_{Total}} * \frac{\%NHCl_2\ (1{:}5{:}25)/100}{2} \quad \text{SE11}$$

$$Reacted\ Cl_{2Form\ NCl_3} = Reacted\ Cl_{2_{Total}} * \frac{\%NCl_3(1{:}5{:}25)/100}{3} \quad \text{SE12}$$

Once the amount of reacted Cl_2 to form a given chloramine has been determined, it is then plotted against the ion counts corresponding to that chloramine. The slope of the linear regression then is defined as sensitivity for each chloramine species with resulting units of ncps/ppbv . To ascertain upper and lower limits in quantitation (manifested through the measurement accuracy) from the sensitivity calculations we assumed the CIMS sensitivity towards all chloramines to be 1:1:1 or 1:5:25 (Figure S10-12).[1,2] A summary of the calculated sensitivities is presented in Table S2. We would expect that the assumed relative sensitivity ratio used in the calculations should be maintained in the final calculated sensitivities between all the chloramines. Using an assumed relative sensitivity of 1:5:25 resulted in calculated calibration sensitivities with relative ratios similar to the assumption (i.e. 1:7.1:22, Table S2). A less comparable outcome was observed when assuming a 1:1:1 relative sensitivity ratio and performing the same check. Therefore, we applied the sensitivities calculated with the 1:5:25 ratio for determining ambient concentrations of all three chloramines. The relative error in the calculated sensitivity (i.e. measurement accuracy) was ±43% for NH_2Cl.

Table S2: Calculated sensitivities for each chloramine species assuming a relative CIMS sensitivity ratio of 1:1:1 or 1:5:25 for NH_2Cl, $NHCl_2$, and NCl_3, respectively. The error reported is one standard deviation (σ) from the regression analysis. See Figure S10-12 for the scatter plots used to determine the sensitivities.

Assumed CIMS Sensitivity Ratio	**NH_2Cl (ncps/ppb)**	**$NHCl_2$ (ncps/ppb)**	**NCl_3 (ncps/ppb)**	**Calculated Sensitivity Ratio (NH_2Cl:$NHCl_2$:NCl_3)**
1:1:1	1160±514	1520±1230	4110±1060	1:1.3:3.5
1:5:25	232±101	1650±1190	5310±7610	1:7.1:22

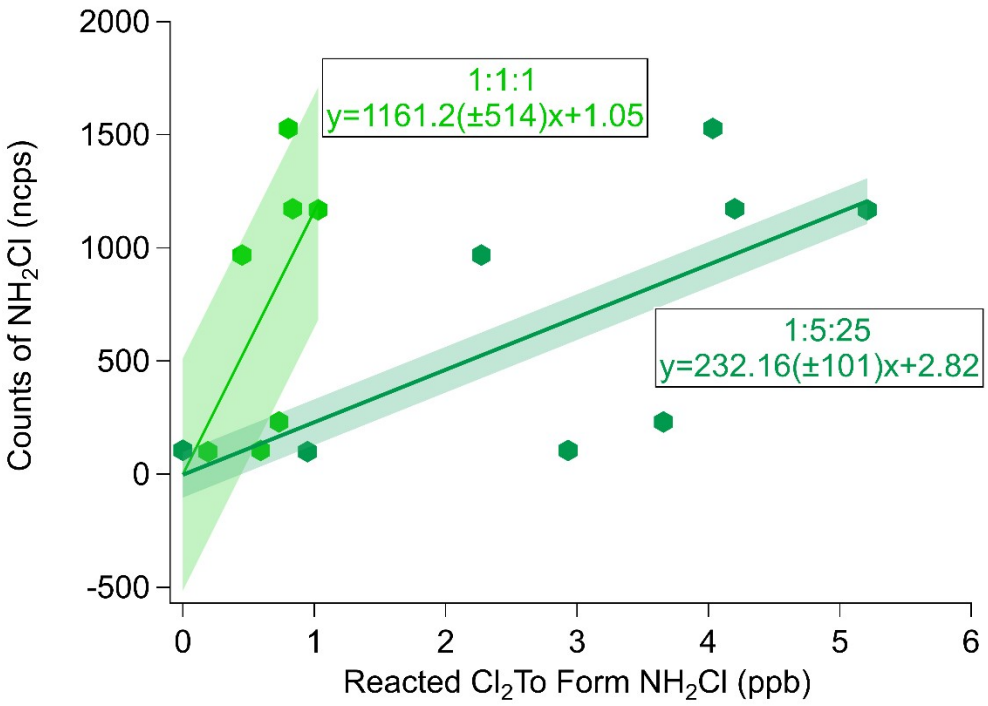

Figure S10: Normalized NH_2Cl counts generated from reaction of Cl_2 to form NH_2Cl (solid line). Regressions using a 1:1:1 (light green) and 1:5:25 (dark green) sensitivities are included as well as the standard deviation (σ) of each slope (shaded area).

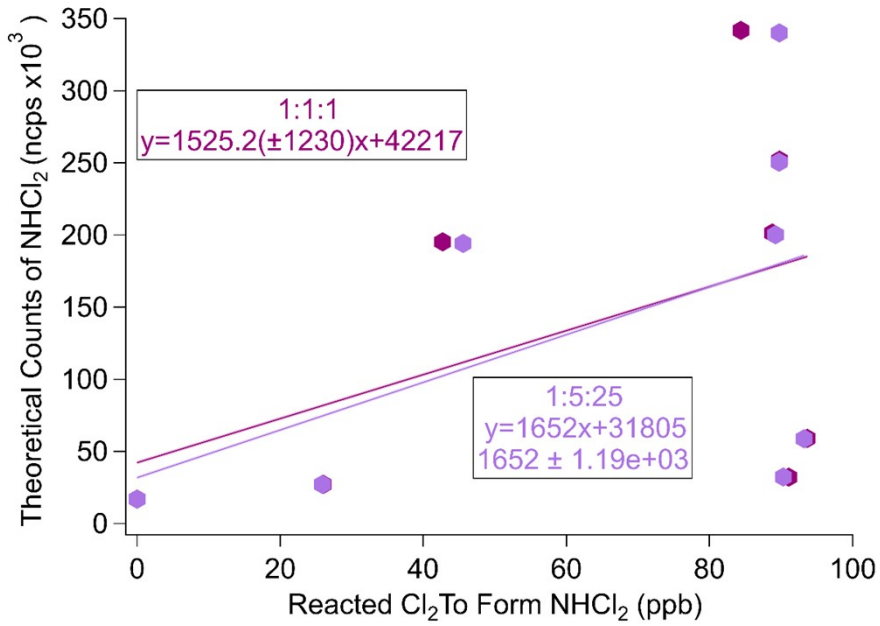

Figure S11: Normalized $NHCl_2$ counts generated from reaction of Cl_2 to form NH_2Cl (solid line). Regressions using a 1:1:1 (light purple) and 1:5:25 (dark purple) sensitivities are included as well as the standard deviation (σ) of the slope (shaded area).

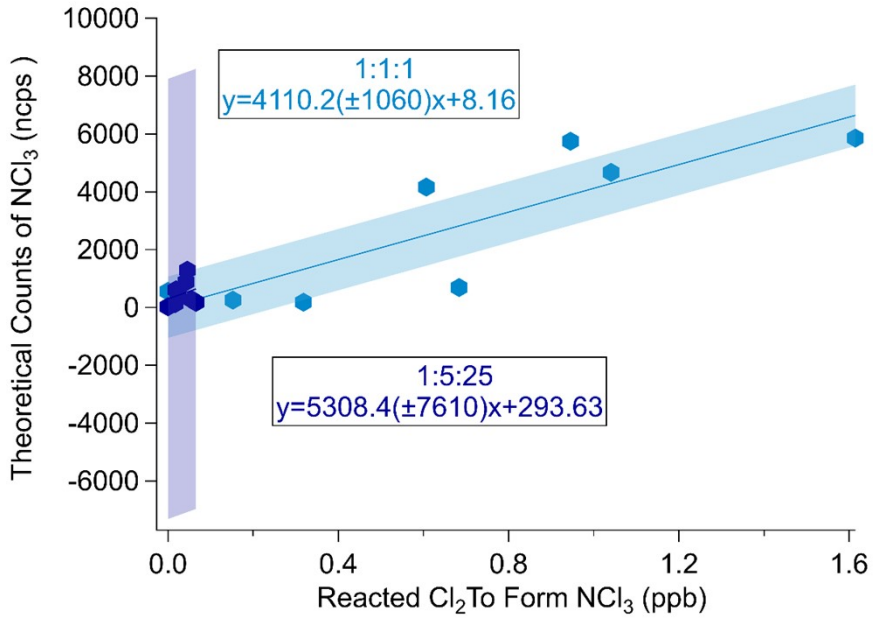

Figure S12: Normalized NCl_3 counts generated from reaction of Cl_2 to form NH_2Cl (solid line). Regressions using a 1:1:1 (light turquoise) and 1:5:25 (dark turquoise) sensitivities are included as well as the standard deviation (σ) of the slope (shaded area).

S5. Isotopic ratios during the calibration experiments

During the calibration experiment, the average isotopic ratios for Cl_2 (197/199) and NH_2Cl (178/180) for the periods of the calibration steps (i.e., the periods with stable measured NH_2Cl and Cl_2 signals, Figure S7) were 1.6±0.005 and 3.6±0.05, respectively (**Figures S13-14**). These isotopic ratios were consistent with the known relative abundance of ^{35}Cl (75%) and ^{37}Cl (25%), further supporting the positive identification of Cl_2 and NH_2Cl (**Table S1**). For Cl_2 the ratio between the three isotopic adducts (i.e. m/z 197, 199, and 201) have a ratio of 9:6:1.

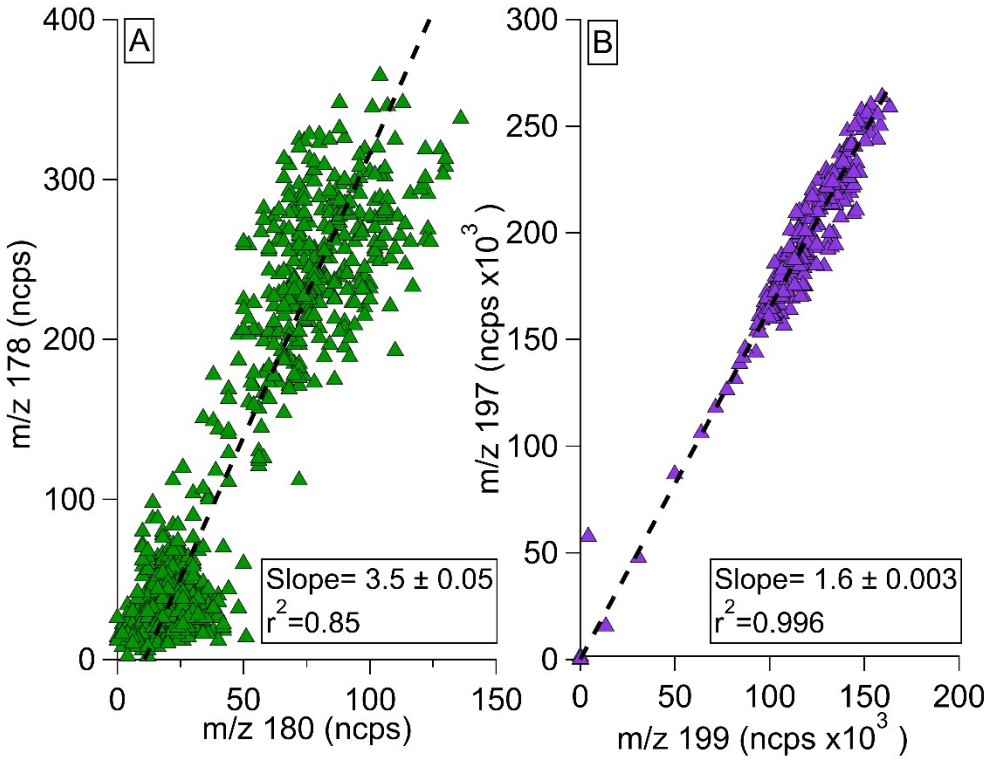

Figure S13: Chlorine isotopic ratio comparisons from the first set of calibration experiments for; (A) $[I{\cdot}ClNH_2]^-$ (178/180) and (B) $[I{\cdot}Cl_2]^-$ (197/199). Correlation coefficient (r^2) values were calculated via orthogonal least-distance regression (black dashed line).

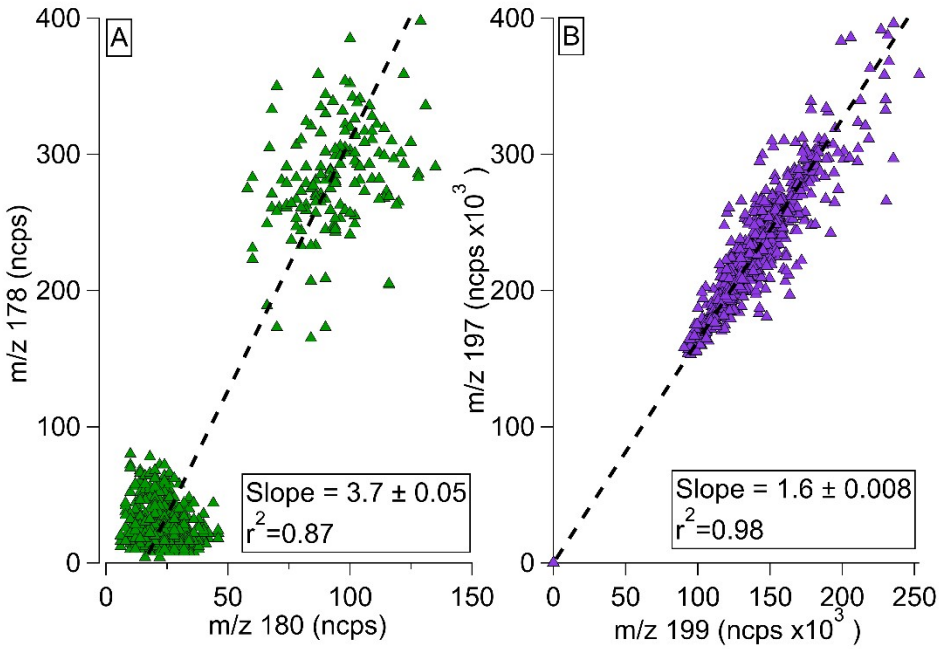

Figure S14: Chlorine isotopic ratio comparisons from the second set of calibration experiments for; (A) $[I{\cdot}ClNH_2]^-$ (178/180) and (B) $[I{\cdot}Cl_2]^-$ (197/199). Correlation coefficient (r^2) values were calculated via orthogonal least-distance regression (black dashed line).

S6. Ambient Measurements: Part 2 - NH_2Cl trends and sources

To estimate the potential impact of emissions from indoor sports complexes on urban air quality, the emission rate of NH_2Cl from indoor sport complexes is needed. We estimated the NH_2Cl emission rate from the University of Leicester Indoor Sport Complex (UL ISC) using a simple gaussian diffusion plume model for point sources (Equation SE13), as outlined in Clarke.[3]

$$Q = \frac{\left(C \cdot \bar{u} \cdot \sqrt{2\pi} \cdot \frac{\pi}{8} \cdot x \cdot \sigma_z\right) + \frac{1h^2}{2\sigma_z^2}}{2e} \qquad \text{SE13}$$

Where Q is the emission rate of the source in μg hr^{-1}, C is the measured concentration of NH_2Cl in μg m^{-3}, $\bar{u}$ is the average wind speed in m hr^{-1}, x is the distance downwind of the plume in m, σ_z is the atmospheric stability term that describes the vertical standard deviation of concentration in m, and h is the source height in m. The atmospheric stability term σ_z was calculated using SE14.[4] We assumed neutral conditions; where I_z=-3.186, J_z=1.1737, K_z=-0.0316, and x is the distance downwind of the plume (40±4 m).

$$\sigma_z = exp(I_z + J_z \ln(x) + K_z[\ln(x)]^2) \qquad \text{SE14}$$

To estimate Q, we used the maximum measured NH_2Cl for selected large plumes during each sampling period, as indicated in Table S3, as these were thought to be representative of direct emissions from the UL ISC. Measured wind speed at the sampling site during each plume was used in the calculation (Table S3). Wind speed data for February 14 and 16 was not available from the AURN station, and so for these dates we assumed the wind speed was the same as February 13 (1.3 m s^{-1}), similar to the mean wind speed for that campaign. The distance between sampling location and the vent on the UL ISC was approximately 40±4 m, and the height of the ventilation exhaust was ca. 4±1 m, and these values were used for x and h, respectively in SE13. The uncertainty associated with the distance to the vent as well as the height of the ventilation create upper (0.41 g hr^{-1}) and lower (0.27 g hr^{-1}) limits of estimated emission rates for UL ISC. This range of estimated emission rates was used to determine the uncertainty in the overall emission calculation (±0.07 g hr^{-1}). Further variability in emission rate between plumes is captured by our analysis of five from each observation period.

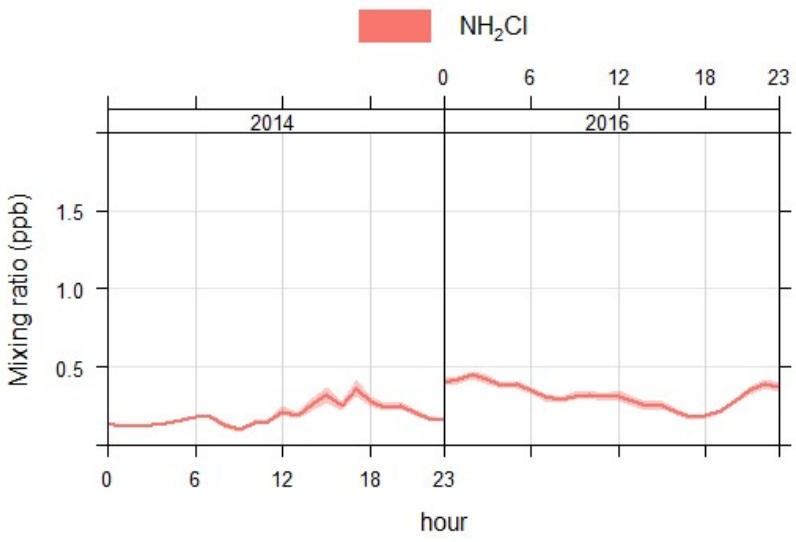

Figure S15: Diurnal trends of NH_2Cl for the 2014 and 2016 sampling periods with shaded areas representing standard deviation(σ). Data has been filtered to be above the LOD (55 pptv). Note that the scale from the full range of observations (Fig 1) is retained here to emphasize that the variability in these diurnal averages over a 24-hour period is likely limited because of the short duration of the observations.

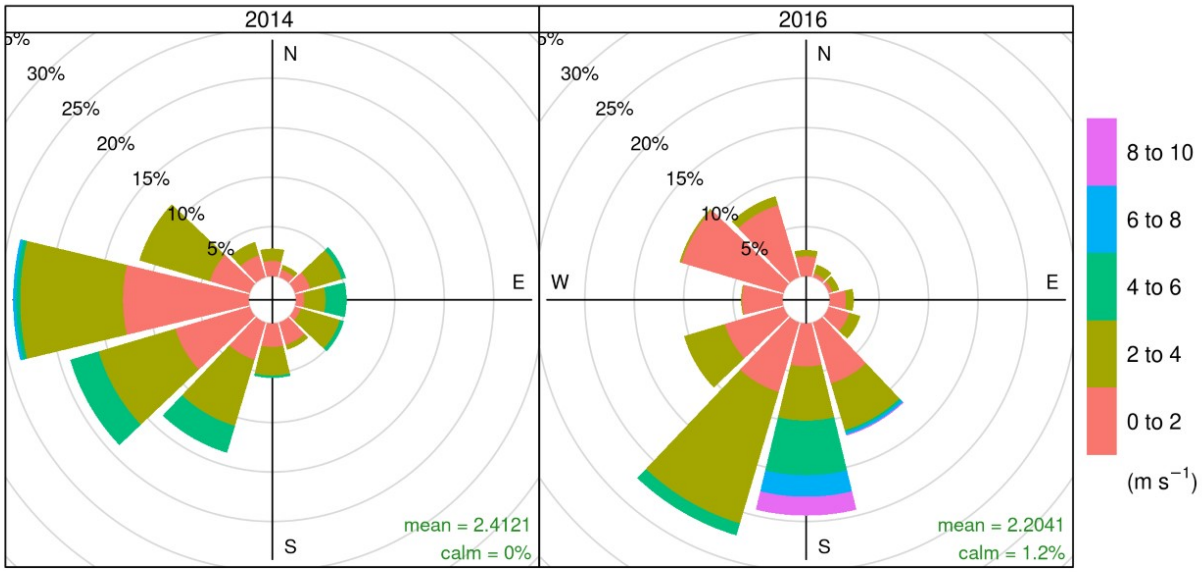

Figure S16: Windrose plots for the 2014 and 2016 sampling periods. Wind direction (radial), percent frequency (axial), and wind speed (m s^{-1}) have been included.

Table S3: Maximum measured NH_2Cl mixing ratios (pptv) and calculate emission rates (g hr^{-1}) for selected large plumes during each sampling period. Emission rates were calculated using SE13.[3] Dates on which measurements were not available are indicated by NA. Error reported for average emission rate is one standard deviation (σ).

Year	Plume Date	Maximum NH_2Cl (pptv)	Wind Speed (m s^{-1})	NH_2Cl Emission Rate (g hr^{-1})	Average NH_2Cl Emission Rate (g hr^{-1})
2014	07-Aug	1300	1.5	0.26	0.35±0.12
	08-Aug	800	1.7	0.19	
	23-Aug	2200	1.5	0.44	
	26-Aug	1400	2.8	0.53	
	27-Aug	650	3.7	0.32	
2016	13-Feb	1700	1.3	0.30	0.32±0.12
	14-Feb	2500	NA	0.44	
	16-Feb	1000	NA	0.17	
	24-Feb	2500	1	0.34	
	26-Feb	1300	2.2	0.38	

References

(1) Chang, C. T.; Liu, T. H.; Jeng, F. T. Atmospheric Concentrations of the Cl Atom, ClO Radical, and HO Radical in the Coastal Marine Boundary Layer. *Environ. Res.* **2004**, *94* (1), 67–74. https://doi.org/10.1016/j.envres.2003.07.008.

(2) Mattila, J. M.; Lakey, P. S. J.; Shiraiwa, M.; Wang, C.; Abbatt, J. P. D.; Arata, C.; Goldstein, A. H.; Ampollini, L.; Katz, E. F.; Decarlo, P. F.; et al. Multiphase Chemistry Controls Inorganic Chlorinated and Nitrogenated Compounds in Indoor Air during Bleach Cleaning. *Environ. Sci. Technol.* **2020**, *54* (3), 1730–1739. https://doi.org/10.1021/acs.est.9b05767.

(3) Clarke, J. F. A Simple Diffusion Model for Calculating Point Concentrations from Multiple Sources. *J. Air Pollut. Control Assoc.* **1964**, *14* (9), 347–352. https://doi.org/10.1080/00022470.1964.10468294.

(4) Seinfeld, J. H.; Pandis, S. N. Atmospheric Diffusion. In *Atmospheric Chemistry and Physics*; 2006; pp 828–899.